POLDER-2 BRDF Database – User Document

Author: Roselyne Lacaze
Date: July 3rd 2006
Ed. 1 - Rev. 1

Content

I. Introduction **4**
II. Instrument and data processing **5**
  II.1 The POLDER data *5*
  II.2 The global land cover data set *5*
  II.3. Methodology for the construction of the BRDF data set *8*
III. Files description **10**
IV. Analysis and discussion **12**
  IV.1. Analysis of the database *12*
  IV.2. Some potential uses of the database *16*
V. Comparison with the POLDER-1 BRDF Database **18**
VI. Conclusion **19**
References **22**
ANNEX 1 : POLDER full resolution reference grid **25**
ANNEX 2 : Examples of BRDFs of neighboring pixels **28**
ANNEX 3 : Examples of multi-temporal BRDFs **41**
ANNEX 4 : BRDFs of mixed pixels. **45**
ANNEX 5 : BRDFs of misclassified pixels **48**
ANNEX 6 : Examples of measured and simulated BRDFs **51**

List of Tables

TABLE 1 : GLOBAL GLC2000 LEGEND WITH ITS VEGETATION CLASSES 6
TABLE 2 : NUMBER OF BRDF FOR EACH GLC2000 CLASS AND EACH MONTH. 12
TABLE 3 : PERCENTAGE OF PIXELS WITH AT LEAST 2 DIFFERENT BRDFS IN THE DATABASE. 14

List of Figures

FIGURE 1: LOCATION OF THE PIXELS SELECTED IN THE POLBER BRDF DATABASE. 13
FIGURE 2: DIRECTIONAL SIGNATURES MEASURED BY POLDER-2 IN THE PRINCIPAL PLANE:1) EVERGREEN NEEDLELEAF FOREST (200307), 2) HERBACEOUS COVER (200306), 3) SHRUB COVER EVERGREEN (200304), 4) SNOW AND ICE (200310). 20

I. Introduction

The Bi-directional Reflectance Distribution Function (BRDF) describes how the terrestrial surfaces reflects the sun radiation. Its potential has been demonstrated for several applications in land surface studies. These includes the correction of bi-directional effects in time series of vegetation indices and reflectances (Leroy and Roujean, 1994; Wu et al., 1995), the direct use of angular measurements for estimation of leaf area index and other biophysical parameters by inversion of radiative transfer models (Knyazikhin et al., 1998; Bicheron and Leroy, 1999), albedo retrieval (Wanner et al., 1997; Cabot and Dedieu, 1997; Capderou, 1998), land cover classifications (Abuelgassim et al., 1996; Bicheron et al., 1997; Hyman and Barnsley, 1997), and radiance to flux conversion factors for Earth radiation budget studies (Manalo-Smith et al., 1998). Then, many users need spatial and temporal variations of the BRDF, for different types of biomes and at different seasons.

The BRDF has been measured in the field (e.g. Kimes, 1983; Deering et al., 1992) or from airborne instruments (Irons et al., 1991; Leroy and Bréon, 1996), with most often an adequate sampling of directional space but with a poor spatial coverage. Directional effects on land surfaces have been seen from space with AVHRR (e.g. Gutman, 1987) or with ATSR (Godsalve, 1995). Then, the spatial coverage is potentially adequate, but the sampling of the BRDF is limited in the angular plane of acquisition. The space-borne POLDER instrument has provided the first opportunity to sample the BRDF of every point on Earth for viewing angles up to 60°-70° , and for the full azimuth range, at a spatial resolution of about 6km, when the atmospheric conditions are favorable (Hautecoeur et Leroy, 1998). POLDER1 has delivered 8 months of global data from November 1996 to June 1997 onboard the Japanese ADEOS-1 platform. A database of 24,857 BRDFs collected at 443, 565, 670, 765 and 865nm has been implemented on the basis of the 22 land cover classes of the GLC2000 land cover classification (GLC, 2003). It is available for downloading on the POSTEL web site (http://postel.mediasfrance.org/Products/BRDF/).

The same methodology has been used to gathered 24,090 BRDFs measured by POLDER2 onboard the ADEOS-2 platform from April to October 2003. The objective is to collect directional information on a maximum number of sites describing the natural variability of continental ecosystems, at several seasons whenever possible, to serve for the development and prototyping of science applications of the BRDF measurement. This document presents the methodology applied for the construction of the BRDF data set, analyzes the database, and describes the files content.

II. Instrument and data processing

II.1 The POLDER data

The POLDER instrument is a radiometer designed to measure the directionality and polarization of the sunlight scattered by the ground atmosphere system. The instrument is made of a bi-dimensional CCD matrix, a rotating wheel that carries filters and polarizers, and a wide field of view lens (114°). The field of view seen by the CCD matrix is ± 43° along track and ± 51° across track. The view zenith angles seen at surface level are larger due to Earth curvature, ± 50 ° along track and ± 61 ° across track (± 70° in the matrix diagonal). The pixel size on the ground is about 6 km for an ADEOS altitude of 800 km. The rotating wheel carries filters that allow spectral measurements at 8 wavelengths (443, 490, 565, 670,763, 765, 865, and 910nm). Three of the channels (443, 670 and 865nm) measure the polarization of the incident light. Images of the same band are acquired every 19.6 s, which permits a large overlap between successive images. During the satellite overpass, a surface target is viewed up to 14 times with each time a different viewing angle. The directional configuration changes each day due to orbital shift between successive days. Therefore, after a few days, assuming favorable atmospheric conditions, the slices of measurements provide a sampling of the BRDF in the limits of the instrument field of view.

The POLDER data are processed to obtain the geocoded, calibrated, cloud screened and atmospherically-corrected land surface reflectances for each orbit. These algorithms consist of a cloud detection, a correction from the effects of absorbing gazes, stratospheric and tropospheric aerosols. Details can be found at www1. Then, a semi-empirical BRDF model (Maignan et al., 2004) is inverted on the directional land surface reflectances acquired during 30-days to assess the directional-hemispherical reflectances, and the anisotropy corrected NDVI. The Leaf Area Index (LAI) and the Fraction of vegetation cover (FVC) are estimated using a neural network which inverts a radiative transfer model. All biogeophysical parameters are produced at a 10-day frequency. Details on these algorithms can be found at www2.

II.2 The global land cover data set

The co-ordination of the Global Land Cover 2000 project has been carried out under the 5th Framework Program 1999-2002 for Research of the European Commission. It is part of the project of the European Commission called Global Environment Information System (GEIS).

In contrast to former global mapping initiatives the GLC2000 project is a bottom up approach to global mapping. In this project more than 30 research teams have been involved, contributing to 19 regional windows. There were two conditions to be fulfilled by the regional experts to guarantee a certain degree of consistency. The data had to be based on SPOT-4 VEGETATION VEGA2000 dataset, which was made freely available by CNE. Secondly, the partners agreed to use the Land Cover Classification System (LCCS) which was provided by FAO (Di Gregorio and Jansen, 2000). The fact that the mapping was carried out by regional experts has a number of benefits. Firstly, since each regional expert has a high level of understanding of their particular region, a certain level of quality can be guaranteed. Secondly, each partner has the freedom to apply their own methods of mapping and define their own regional legend. This allows the partners to apply the classification techniques they find most appropriate for land cover mapping in their respective region. Thirdly, the regional mapping approach ensures that access could be gained to reference material. For more information on the partners and the production of the regional products go to the web site (www3) and consult the metadata database www4 under the topic "description".

N°	Global Land Cover Class
1	Tree Cover, broadleaved, evergreen
2	Tree Cover, broadleaved, deciduous, closed
3	Tree Cover, broadleaved, deciduous, open
4	Tree Cover, needle-leaved, evergreen
5	Tree Cover, needle-leaved, deciduous
6	Tree Cover, mixed leaf type
7	Tree Cover, regularly flooded, fresh
8	Tree Cover, regularly flooded, saline, (daily variation)
9	Mosaic: Tree cover / Other natural vegetation
10	Tree Cover, burnt
11	Shrub Cover, closed-open, evergreen (with or without sparse tree layer)
12	Shrub Cover, closed-open, deciduous (with or without sparse tree layer)
13	Herbaceous Cover, closed-open
14	Sparse Herbaceous or sparse shrub cover
15	Regularly flooded shrub and/or herbaceous cover
16	Cultivated and managed areas
17	Mosaic: Cropland / Tree Cover / Other Natural Vegetation
18	Mosaic: Cropland / Shrub and/or Herbaceous cover
19	Bare Areas
20	Water Bodies (natural & artificial)
21	Snow and Ice (natural & artificial)
22	Artificial surfaces and associated areas

Table 1 : Global GLC2000 legend with its vegetation classes

The regional legends are compatible with the LCCS, which describes land cover according to a hierarchical series of classifiers and attributes. These separate vegetated or non-vegetated surfaces; terrestrial or aquatic/flooded; cultivated and managed; natural and semi-natural; life-form; cover; height; spatial distribution; leaf type and phenology. Coding each class with LCCS allows a map legend to be progressively more detailed for regional, and in some cases, national level users. Due to its hierarchical structure it is possible to translate the regional classification into a more general one – the global legend (Table 1).

First, the GLC2000 classification, available at 1/120° space resolution in a regular latitude/longitude grid, has been resampled to 1/18° space resolution. Specific aggregation rules have been defined:

- The majority class on the "1/18° "area is allocated to the resulting pixel
- In case of equality between two or many classes, the class is assigned to the resulting pixel in the following priority order:
  - Water Bodies
  - Snow and Ice
  - Artificial Surfaces
  - Bare Areas
  - Mosaic: Cropland / Tree Cover / Other natural vegetation
  - Mosaic: Cropland / Shrub and / or Herbaceous cover
  - Mosaic: Tree cover / Other natural vegetation
  - Cultivated and managed areas
  - Regularly flooded shrub and /or herbaceous cover
  - Tree Cover, regularly flooded, saline
  - Tree Cover, regularly flooded, fresh
  - Sparse Herbaceous or sparse shrub cover
  - Shrub Cover, closed-open, deciduous
  - Shrub Cover, closed-open, evergreen
  - Herbaceous Cover, closed-open
  - Tree Cover, burnt
  - Tree Cover, mixed leaf type
  - Tree Cover, broadleaved, deciduous, open
  - Tree Cover, broadleaved, deciduous, closed
  - Tree Cover, needled-leaved, deciduous

- Tree Cover, broadleaved, evergreen
- Tree Cover, needle-leaved, evergreen

This order choose the non-vegetated classes, first, and then, the other classes according to their “mixity level”, since most of the resulting pixels are mixed areas. That allows to insure a larger “pureness” to forest areas, which usually display the most specific BRDFs.

Then, the re-sampled map has been re-projected in the sinusoidal POLDER grid using the nearest neighbor method. At final, as the GLC_2000 classification is truncated at 56° South, the map has been filled to South pole using the IGBP classification.

II.3. Methodology for the construction of the BRDF data set

The basic inputs for the construction of the BRDF data set is level 2 bi-directional surface reflectances at 443, 565, 670, 765 and 865nm over the 7 months of POLDER-2 acquisition. The pixels are classified according:

- The 22 biomes of the GLC2000 classification.
- The period of measurement (YYYYMM) where YYYY corresponds to the year and MM to the month of acquisition.
- The NDVI from level 3 synthesis product. We use the period of composition centered on 15^{th} of the considered month. Values of NDVI are classified in 12 classes from –0.2 to 1 with a step equal to 0.1.
- The location of the pixel in 5 bands of latitude (90° N-50° N; 50° N-30° N; 30° N-30° S; 30° S-50° S; 50° S-90° S) (AREA)

The criteria of selection for the pixels are:

1. The number of view on the track shall be higher or equal to 10.
2. The distribution of tracks in the viewing hemisphere. This one is sampled by 8° and the tracks, characterized by the viewing zenith angle of their center, are distributed in the corresponding directional classes. A pixel shall have at least one track in 5 different angular classes during the considered month to be selected.
3. The number of clear tracks collected during the considered month shall be higher or equal to 8.

At the most, 10 pixels (the best according the number of directional classes and tracks) are selected for each of the 10560 (22*8*5*12) GLC-YYYYMM-AREA-NDVI classes. Then, the filtering algorithm of the Level 3 “Land Surface” POLDER-2 processing line is applied (Lacaze, 2005). It allows removing the residual cloudy tracks and data perturbed by a high content of aerosols using a temporal analysis of directional observations acquired close to the perpendicular plane. We keep only pixels for which the previous criteria 2 and 3 shall remain valid after filtering. At final, 24,090 pixels frame the database.

III. Files description

Directories tree reproduces the classification applied on the POLDER pixels:

- The directories are GLC_XX where XX is the biome class in the GLC2000 classification.
- The subdirectories are YYYYMM corresponding to the year (YYYY) and the month (MM) of acquisition.

The BRDF files (brdf_ndviXX.LLLL_CCCC.dat) are compound by:

- the class of NDVI, XX (01 correspond to the interval [-0.2, -0.1] and 12 to the interval [0.9, 1]
- The location of the pixel in the standard POLDER grid at full resolution (LLLL: line and CCCC: column) (see Annex 1)

The BRDF files are ASCII files presented in a columnar format. The C format used is the following: "%4d %8.3f %8.3f %8.3f %8.3f %8.3f %8.3f %8.3f %8.3f %8.3f\n». The "no data" value is NaN. The different fields are:

dd tetas phis tetav phi r443 r565 r670 r765 r865

where:

dd	: day of the month (1-31)
tetas	: solar zenith angle (°)
phis	: solar azimuth angle (°)
tetav	: view zenith angle (°)
phi	: relative azimuth angle (°)
r443	: surface reflectance observed at 443nm
r565	: surface reflectance observed at 565nm
r670	: surface reflectance observed at 670nm
r765	: surface reflectance observed at 765nm
r865	: surface reflectance observed at 865nm

Warning: *One month corresponds to a period of synthesis, which is 429 overpass, and not to a calendar month. Then, some side effects can appear for months where the number of days are low (e.g. February).*

Two additional files are provided:

- the final classification derived from re-sampled and re-projected GLC2000 map (landcover_map.bin)
- the number of 1/120° resolution pixels, belonging to the final class, and present on the 1/18° resolution pixel.(nbpixel_map.bin)

These maps are presented in the POLDER full resolution grid (Annex 1). Values are coded on one byte.

IV. Analysis and discussion

The 24,090 BRDFs are shared between the 22 GLC2000 classes and the 7 months following the distribution presented in the Table 2.

	200304	200305	200306	200307	200308	200309	200310	Total
GLC_01	109	95	69	79	90	106	69	**617**
GLC_02	168	198	181	171	163	188	145	**1214**
GLC_03	147	103	88	125	106	138	79	**786**
GLC_04	197	195	246	300	292	259	222	**1711**
GLC_05	86	93	123	127	110	88	75	**702**
GLC_06	179	179	155	186	175	201	181	**1256**
GLC_07	12	27	19	39	30	10	14	**151**
GLC_08	37	34	13	21	13	30	14	**162**
GLC_09	105	138	139	206	192	163	127	**1070**
GLC_10	90	67	111	108	98	78	63	**615**
GLC_11	161	164	204	281	234	205	178	**1427**
GLC_12	209	225	233	281	214	226	202	**1590**
GLC_13	185	211	223	261	215	240	223	**1558**
GLC_14	183	183	226	251	232	237	201	**1513**
GLC_15	134	185	208	194	185	190	168	**1264**
GLC_16	201	204	180	196	184	227	220	**1412**
GLC_17	126	155	125	145	124	142	110	**927**
GLC_18	165	189	184	176	175	174	150	**1213**
GLC_19	164	158	208	229	179	206	140	**1284**
GLC_20	239	246	267	309	271	293	264	**1889**
GLC_21	47	58	69	157	127	174	50	**682**
GLC_22	172	139	137	163	127	177	132	**1047**
Total	**3116**	**3246**	**3408**	**4005**	**3536**	**3752**	**3027**	**24090**

Table 2 : Number of BRDF for each GLC2000 class and each month.

IV.1. Analysis of the database

Figure 1 displays the spatial distribution of the selected pixels. Very few of them are located in the equatorial region because of the dense cloud cover, and in China. As the measurements were acquired during the summer of Northern hemisphere, the Europe, Eurasia and North America are very well sampled, especially at high latitude. The sampling is strongly marked by the short orbit cycle of ADEOS-2 (4 days).

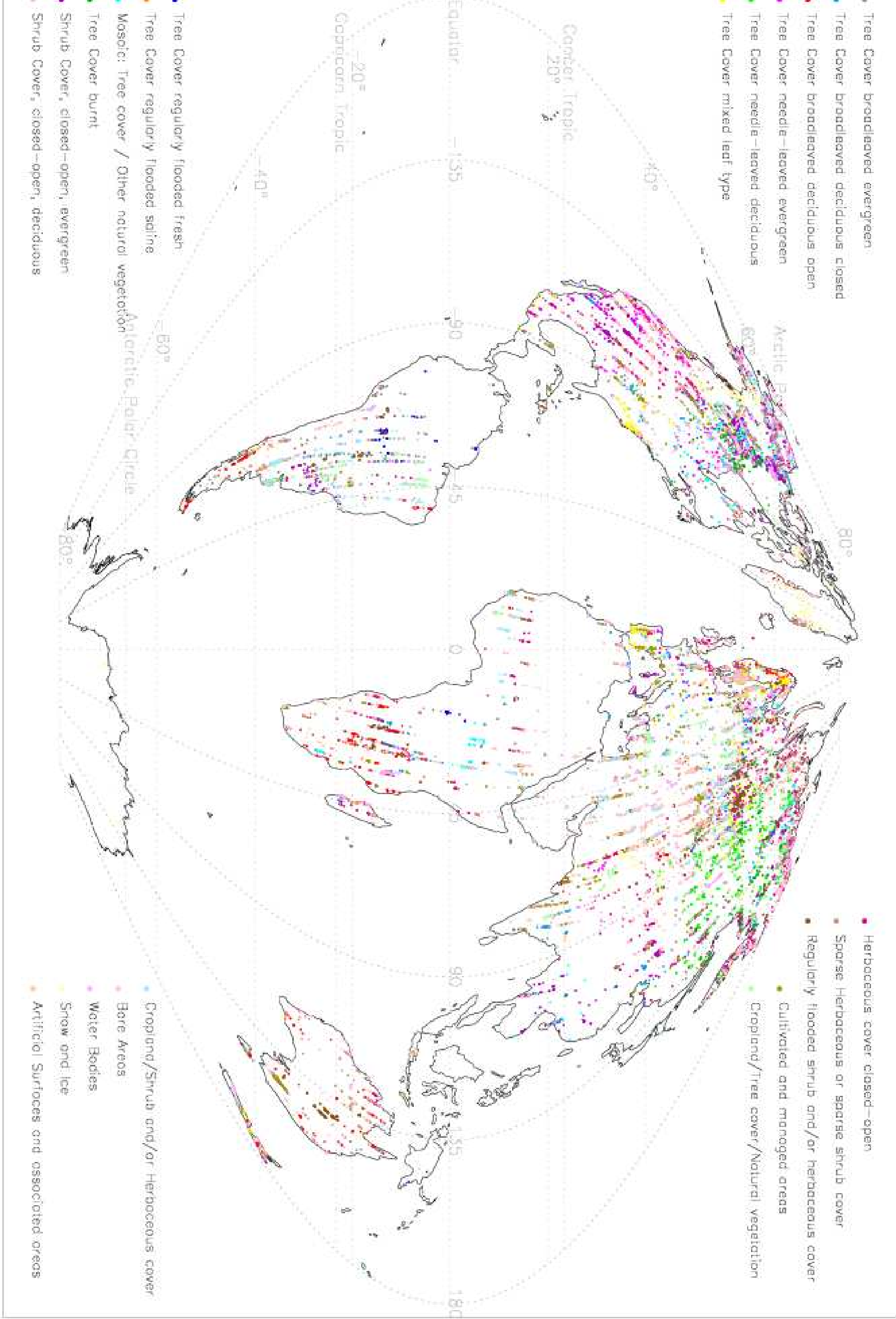

Figure 1: Location of the pixels selected in the POLBER BRDF database.

GLC 2000 Class	% of pixels
01	12.3
02	10.9
03	12.6
04	13.1
05	3.7
06	13.1
07	21.2
08	24.7
09	12.3
10	14.3
11	13.2
12	9.1
13	9.0
14	9.3
15	14.2
16	10.8
17	16.7
18	15.0
19	12.7
20	11.1
21	16.1
22	23.3
All classes	**12.5**

Table 3 : Percentage of pixels with at least 2 different BRDFs in the database.

In each GLC_XX/YYYYMM section, we can note many clumps of 3, 4 or even more neighboring pixels. Indeed, when one pixel answers the criteria of selection, it's highly likely that its neighbor does also. This clustering of BRDFs is illustrated for various vegetation types and different NDVI ranges in Annex 2. Figures show that the BRDFs of each neighboring pixel are very similar. They present the same trends: a maximum of reflectance when the solar and the viewing directions coincide (the hot spot effect); a minimum of signal in the forward scattering directions; equal values of reflectance for a given waveband. Annex2_11 shows BRDFs of neighboring water pixels located on a lake. Figures display low reflectance values except in the glitter direction where the BRDF presents a sharp peak which magnitude is quite the same in all wavebands. Snow cover exhibit very high reflectances, especially in the visible wavebands (Annex2_12). The BRDFs display an increase of values in the forward scattering direction. In a general way, the BRDFs at 443nm appear quite noisy because of the great impact of the atmosphere in this spectral band. At 565nm, 670nm and 865nm, the BRDFs display regular features in spite of the natural variations of the surface during the 30 days of acquisitions. That proves the ability of POLDER sensor to accurately measure the surface anisotropy.

The database contains some pixels selected at several months. The Table 3 gives the percentage of pixels of each GLC class having at least 2 different BRDFs. This allows monitoring the temporal evolution of the surface. Annex 3 presents the multi-temporal BRDFs of different vegetation types. An evergreen shrubland that doesn' t change during the year: the NDVI class remains constant with values between [0.3, 0.4] and the reflectances stay quite stable (Annex3_1). The major changes in the BRDFs are due to the variations of the sun angle. We can also note a high reflectance in the glitter direction in September. That translates the presence of a temporary water body in the pixel. The second example shows BRDF from May to September of a broadleaf deciduous forest located in Alaska (Annex3_2). The vegetative cycle is translated by variations of the spectral reflectances: the strong increase of NDVI from May to June yields a decrease of red reflectance and an increase of the near-infrared values. The opposite trend appears from August to September. In May and August, the BRDF display a peak of reflectance in the glitter direction. A small lake is probably present in the pixel area. Annex3_2 shows BRDFs of a cultivated pixel in Canadian great plains. The maximum of NDVI in July is linked to the lowest red reflectances and the highest near-infrared values.

Because most of the POLDER pixels are mixed areas, and on account of aggregation rules for classification re-sampling, some inconsistencies can appear between the class name and the BRDF aspect or the NDVI value. In these cases, the companion file containing the number of “1/112° ” resolution pixels belonging to the final class and present on a POLDER pixel, can help to have an idea of the pureness level of the pixel. For example, Annex4_1 shows a pixel classified in “Water Bodies”, which should display low reflectances. Actually, it displays a vegetative cycle with NDVI variations from 0.5 to 0.7 between April and August, and BRDF features characterizing a vegetation area. The *nbpixel_map.bin* file indicates that only 60% of the original 1/112° resolution pixels inside this POLDER pixel belong to the “Water Bodies” class. The presence of water is translated by a high reflectance in the glitter direction, which is, however, lower than the reflectance in the hot spot direction. A second example is presented in Annex4_2. These neighboring pixels located in Iran are classified in “Bare Areas”, but the NDVI values are in the range [0.5, 0.7]. We can note different aspects of visible BRDFs between Northern pixels whose NDVI is from 0.5 to 0.6, and Southern pixels whose NDVI is from 0.6 to 0.7. The first ones display typical BRDFs of bare soil, as where as the latter ones display vegetation BRDFs, with low reflectances in the visible bands, even in the hot spot direction. In the near-infrared band, the BRDFs are very similar. These pixels are mixed areas located at the transition between “bare area”, at North, and a “shrub cover, deciduous” region at South. The relative part of soil and vegetation is clearly visible in the BRDF shape.

Some pixels are also misclassified clearly. In Annex5_1, we can see an example of neighboring pixels identified as "Burnt Areas", that should display low reflectances. However the NDVI is high, between [0.7-0.8], and the BRDFs are typical of a green vegetation, with a sharp peak in the hot spot direction. We can assume that the vegetation has grown again between 2000, when the data used to made the land cover map has been collected, and 2003 when the POLDER-2 measurements have been acquired. Likewise, Annex5_2 displays multi-temporal BRDFs of pixel identified as a broadleaf evergreen forest. However, the NDVI is low, between [0.1, 0.2], and the reflectances high in the visible bands. The *nbpix_map.bin* file indicates that less than 50% of the 1/112° resolution pixels belong to the “broadleaf evergreen forest” class. According to the directional features, we can assume that this pixel located in the high plateau of Peru is probably a sparse vegetation area, whose soil has a strong impact on the BRDF.

IV.2. Some potential uses of the database

The BRDFs of the database provide detailed information about the angular properties of the land surface ecosystems. Measurements acquired in the principal plane, where the BRDFs display its sharpest features, show the great potential of these data. As examples, figure 2 presents spectral directional signatures of 4 various ecosystems at different time periods. The graphs show that reflectances at 565nm are higher than reflectances at 670nm for vegetation (Evergreen needleleaf forest, Herbaceous Cover). When the influence of soil background increases, the reflectance at 670nm is closer to the reflectance at 565nm (Shrub Cover Evergreen). The main pattern of the BRDF is the peak of reflectance in the hot spot direction. Its width and magnitude vary according to the ecosystems. This BRDF feature can be very useful to retrieve structural parameters of the vegetation or to quantify the spatial distribution of the major elements of the landscape. Such approaches have already be investigated by Lacaze et al. (2002), Chen et al. (2003), and Leblanc et al. (2005). The BRDF of Snow and Ice (Figure 2d) displays well distinct spectral profiles with maximum of reflectances at 443nm and minimum in the near-infrared. The specific bowl shape shows an increase of reflectance in the forward direction, which translates the presence of a thin water layer at the surface. The directional profiles are strongly marked by the POLDER-2 short cycle (4 days). The scattering of reflectances for a given viewing configuration translates the variation of surface during the synthesis period. On Figure 2, the pixels are quite stable over one month. The impact of changes in illumination angles can be neglected, except around the hot spot direction where the variations of reflectances are maxima.

Above all, the POLDER BRDF database is a unique and essential tool for testing the abilities of radiative transfer models to simulate the directional properties of the surface with the aim, for instance, to correct the bi-directional effects. Such application can be achieved with the linear reflectance model of Maignan et al. (2004), which is used in the algorithm of “Land Surface” processing line to normalize the POLDER data (www2). Annex 6 presents examples, one for each GLC2000 class, of the measured BRDF, the simulated one after inversion of the Maignan model, and a scatter-plot comparing the both for 3 wavebands. The quality of the inversion depends on the ecosystem and its specificities. The model reproduces the sharp peak of reflectance of the hot spot phenomenon very well (e.g. Annex6_4, Annex6_5, Annex6_11 or Annex6_17) because of the hotspot module (Bréon et al., 2002) merged with the Ross_thick kernel. The model cannot simulate the glitter effect when some water is on the surface (Annex6_7, Annex6_8, Annex6_20). The model is well adapted to simulate the directional reflectances of discontinuous landscapes (e.g. Annex6_12, Annex6_14, Annex6_15, Annex6_18 or Annex6_22). The best results of the inversion are obtained in the near infrared channel where the multiple scattering smoothes the directional features of the BRDF.

V. Comparison with the POLDER-1 BRDF Database

This part will be completed in the next months.

VI. Conclusion

With the existing POLDER-1 BRDFs database, these POLDER-2 BRDFs are an exceptional collection of bi-directional reflectances measured from space, providing exclusive information about the anisotropy of the continental ecosystems. What makes it an incomparable tool for many environmental studies.

Another database will be generated in the next months with the PARASOL/POLDER-3 BRDFs.

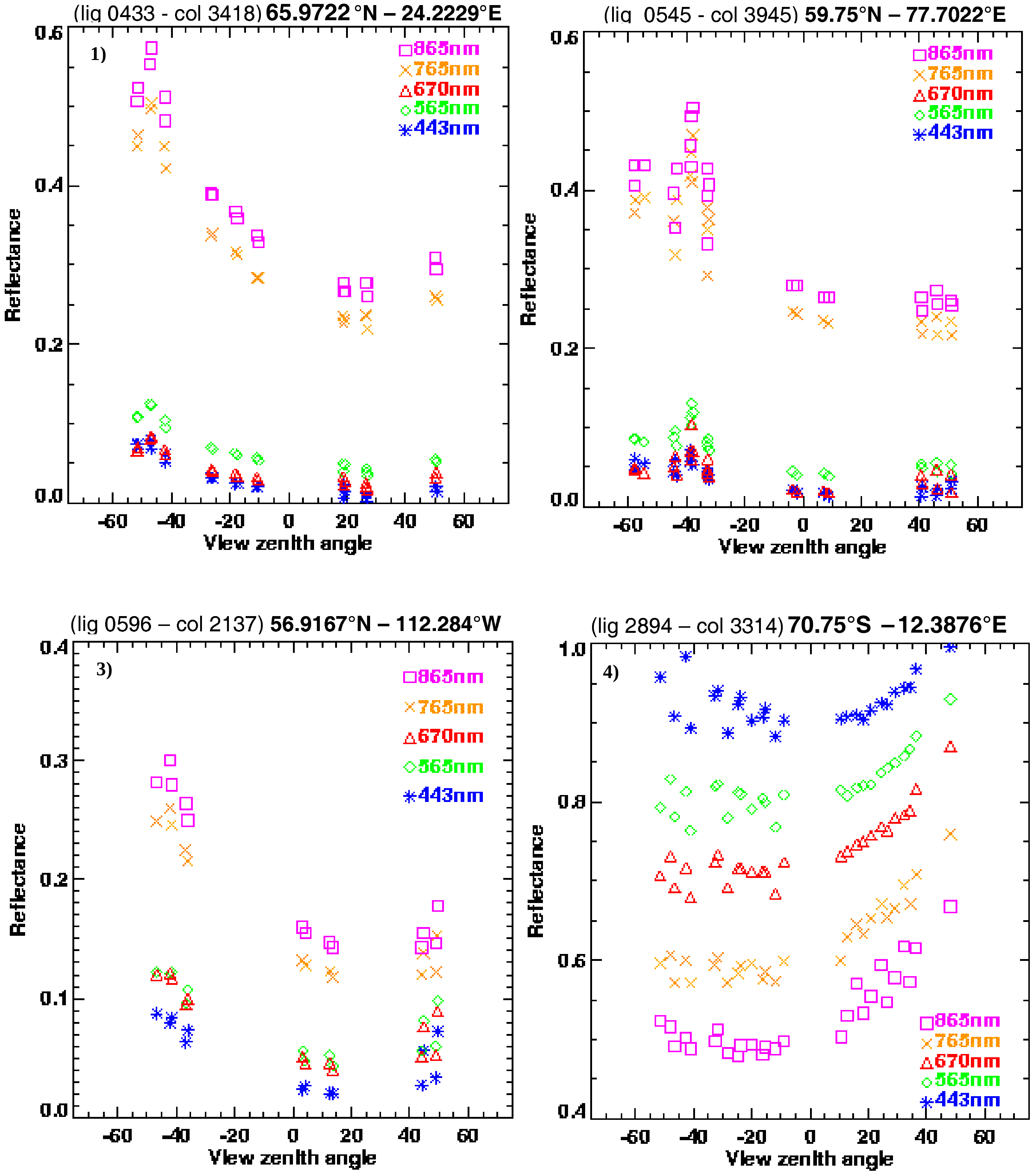

Figure 2: Directional signatures measured by POLDER-2 in the principal plane:1) Evergreen Needleleaf Forest (200307), 2) Herbaceous Cover (200306), 3) Shrub Cover Evergreen (200304), 4) Snow and Ice (200310).

Acknowledgment

The BRDF monthly synthesis database from POLDER-2/ADEOS-2 measurements version 1.0 (March 25th, 2006) has been produced by POSTEL, the pole of thematic competences on Land Surfaces. The POLDER-2/ADEOS-2 data are from Cnes/NASDA.

The original tools used to test the potential of the BRDF database for model inversion has been developed by F-M. Bréon (CEA/LSCE). The Annex 1 is extracted from the “POLDER Level-1 Product Data Format and User Manual“ prepared by F-M. Bréon (CEA/LSCE) with the collaboration of CNES Project Team and available in the Documentation page of the POLDER web site http://polder.cnes.fr.

For any questions, please contact:

Dr. R. Lacaze
Medias-France
CNES bpi 2102
18, avenue Edouard Belin
31401 Toulouse Cedex 9
France

Phone: 33-5-61-27-31-21
Fax: 33-5-61-28-29-05
Email: roselyne.lacaze@medias.cnes.fr

References

Global Land Cover 2000 database. European Commission, Joint Research Centre, 2003, www3.

Abuelgasin, A., S. Gopal, J. R. Irons, and A. H. Strahler, Classification of ASAS multiangle and multispectral measurements using artificial neural networks, *Remote Sensing of Environment, 57, 79-87,* 1996.

Bicheron, P., M. Leroy, O. Hautecoeur, and F. M. Bréon, Enhanced discrimination of boreal forest covers with directional reflectances from the airborne polarization and directionality of Earth Reflectances (POLDER) instrument, *Journal of Geophysical Research, 102, 29,517-29,528,* 1997.

Bicheron, P. and M. Leroy, A method of biophysical parameter retrieval at global scale by inversion of a vegetation reflectance model, *Remote Sensing of Environment, 67, 251-266,* 1999.

Bicheron, P. and M. Leroy, Bidirectional reflectance distribution function signatures of major biomes observed from space, *Journal of Geophysical Research, 105, 21, 26,669-26,681,* 2000.

Bréon, F.M. , F. Maignan, M. Leroy, and I. Grant, Analysis of the hot spot directional signatures measured from space, *Journal of geophysical research, 107, (16), 4,282-4,296,* 2002.

Cabot, F. and G. Dedieu, Surface albedo from space: Coupling bidirectional models and remotely sensed measurements, *Journal of Geophysical research, 102, 19,645-19,664,* 1997.

Capderou, M. , Determination of the shortwave anisotropic function for clear sky desert scenes from ScaRab data: Comparison with models issued from other satellite data, *Journal of Applied Meteorology, 37, 1398-1411,* 1998.

Chen, J.M., J. Liu, S.G. Leblanc, R. Lacaze, and J.L. Roujean, Multi-angular optical remote sensing for assessing vegetation structure and carbon absorption, *Remote Sensing of Environment, 84, Issue 4, 516-525*, 2003.

Deering, D. W., T. F. Eck and T. Grier, Shinnery oak bidirectional reflectance properties and canopy model inversion, *IEEE Transaction in Geoscience and Remote Sensing, 30, 339-348,* 1992.

Di Gregorio, A. and Jansen, L., Land Cover classification system, classification concepts and user manual, *Food and Agriculture Organisation of the United Nations: Rome,* 2000.

Godsalve, C., Bidirectional reflectance sampling by ATSR-2: A combined orbit and scan model, *International Journal of Remote Sensing, 16, 269-300,* 1995.

Gutman, G. G., the derivation of vegetation indices from AVHRR data, *International Journal of Remote Sensing, 8, 1235-1243,* 1987.

Hautecoeur, O. and M. Leroy, Surface bidirectional reflectance distribution function observed at global scale by OLDER/ADEOS, *Geophysical Research Letter, 25, 4197-4200,* 1998.

Hyman, A. H., and M. J. Barnsley, On the potential for land cover mapping from multiple view angle (MVA) remotely sensed information, *International Journal of Remote Sensing, 18, 2471-1475,* 1997.

Irons, J. R., K. J. Ranson, D. L. Williams, R. R. Irish, and F. G. Huegel, An off-nadir pointing imaging spectroradiometer for terrestrial ecosystem studies, *IEEE Transaction in Geoscience and Remote Sensing, 29, 66-74,* 1991.

Kimes, D. S., Dynamics of directional reflectance factor distributions for vegetation canopies, *Applied Optics, 22, 1364-1373,* 1983.

Knyazikhin, Y., J. V. Martonchik, D. J. Diner, R. B. Myneni, M. M. Verstraete, B. Pinty, and N. Gobron, Estimation of vegetation canopy leaf area index and fraction of absorbed photosynthetically active radiation from atmosphere-corrected MISR data, *Journal of Geophysical Research, 103, 32,239-32,256,* 1998.

Lacaze, R., J. M. Chen, J. L. Roujean and S. G. Leblanc, Retrieval of vegetation clumping index using hot spot signatures measured by POLDER instrument, *Remote Sensing of Environment, 79, 84-95,* 2002.

Lacaze, R, POLDER-2 Land Surface Level-3 Products, User Manual, Algorithm Description and Product Validation, *Medias-France, Issue 1, Revision 4*, August 25th 2005 (www5).

Leblanc, S.G., J.M. Chen, H.P. White, R. Latifovic, R. Lacaze, and J.L. Roujean, Canada-wide foliage clumping index mapping from multi-angular POLDER measurements, *Canadian Journal of Remote Sensing, in press,* 2005.

Leroy, M and J. L. Roujean, Sun and view angle corrections on reflectances derived from NOAA/AVHRR data, *IEEE Transaction in Geoscience and Remote Sensing, 32, 684-697,* 1994.

Leroy, M. and F. M. Bréon, Surface reflectance angular signatures from airborne POLDER data, *Remote sensing of environment, 57, 97-107,* 1996.

Loveland, T. R. and A. S. Belward, The IGBP-DIS global 1-km land cover data set DISCover: first results, *International Journal of Remote Sensing, 18, 3289-3295,* 1997.

Maignan, F., F.M. Bréon, et R. Lacaze, Bidirectional reflectance of Earth targets : evaluation of analytical models using a large set of spaceborne measurements with emphasis of the hot spot, *Remote Sensing of Environment, vol.90, 210-220*, 2004.

Manalo-Smith, N., G. L. Smith, S. N. Tiwari, and F. W. Taylor, Analytic form of bidirectional reflectance functions for application to Earth radiation budget studies, *Journal of Geophysical Research, 103, 19,733-19,751,* 1998.

Wanner, W., A. H. Strahler, B. Hu, P. Lewis, J. P. Muller, X. Li, C. L. Barker Schaaf, and M. J. Barnsley, Global retrieval of bidirectional reflectance and albedo over land from EOS MODIS and MISR data: Theory and algorithm, *Journal of Geophysical Research, 102, 17,143-17,161,* 1997.

Wu, A., Z. Li and J. Cilhar, Effects of land cover type and greenness on advanced very high radiometer bidirectional reflectances: Analysis and removal, *Journal of Geophysical Research, 100, 9179-9192,* 1995.

www1 : http://smsc.cnes.fr/POLDER/SCIEPROD/lsp2algol2.htm
www2 : http://smsc.cnes.fr/POLDER/SCIEPROD/lsp2algol3.htm
www3 : http://www.gvm.jrc.it/glc2000.
www4 : http://www.gvm.jrc.it/glc2000/Products/fullproduct.asp
www5 : http://postel.mediasfrance.org/Download/